

## Frequency-dependent ferroelectric and electrocaloric properties in barium titanate-based ceramics based on Maxwell relations

Wanting Shu\*, Hong Li\*, Yanli Huang<sup>†,‡</sup>, Cong Lin<sup>†</sup>, Xiao Wu<sup>†</sup>, Min Gao<sup>†</sup>,  
Tengfei Lin<sup>†</sup> and Chunlin Zhao<sup>†,§</sup>

\*College of Materials Science and Engineering  
Fuzhou University, Fuzhou 350108, P. R. China

<sup>†</sup>College of Photonic and Electronic Engineering  
Fujian Normal University, Fuzhou 350117, P. R. China

<sup>‡</sup>yanlihuangylh@163.com  
<sup>§</sup>zhaochunlin@fzu.edu.cn

Received 2 January 2024; Revised 11 February 2024; Accepted 4 March 2024; Published 26 March 2024

In this work, the frequency dependence of ferroelectric and electrocaloric properties in barium titanate-based ceramics was studied based on Maxwell relations. It is found that the maximum and remnant polarization will decrease while the coercive field increases a lot with rising frequency from 0.1 to 10 Hz, indicating that polarization rotation and domain switching become difficult at high frequencies. The electrocaloric properties show the different frequency dependence at different phase structures. Isothermal entropy change ( $\Delta S$ ) and adiabatic temperature change ( $\Delta T$ ) are similar around/above Curie temperature ( $T_C$ ), showing tiny frequency dependence. However,  $\Delta S$  and  $\Delta T$  display the obvious frequency dependence below  $T_C$ , especially in the orthorhombic–tetragonal phase-transition region with a stable ferroelectric phase, and this frequency dependence becomes more obvious under a low-electric field. It is also found that increasing the frequency can weaken the electric field dependence of electrocaloric strength. This work gives a general profile of frequency dependence for electrocaloric properties in ferroelectric ceramics.

**Keywords:** Electrocaloric properties; ferroelectric ceramics; barium titanate; frequency dependence.

### 1. Introduction

The electrocaloric effect represents a phenomenon of temperature change or entropy change induced by the change of polar order parameters by applying an external electric field in a polar material.<sup>1–4</sup> The high electrocaloric effect is usually obtained in ferroelectric materials due to the presence of numerous spontaneous polarizations within the ferroelectrics.<sup>5–9</sup> Based on the electrocaloric effect of ferroelectrics, the electrocaloric cooling technology can be developed, which shows the merits of high energy efficiency, weak greenhouse effect and capability on device miniaturization and this can be applied as the next-generation environmental-friendly cooling technology.<sup>2</sup> Based on the Maxwell relation,  $(\partial P/\partial T)_E = (\partial S/\partial E)_T$ , the phenomenological expressions of the electrocaloric effect can be obtained<sup>10–12</sup>:

$$\Delta S = \frac{1}{\rho} \int_{E_1}^{E_2} \left( \frac{\partial P}{\partial T} \right)_E dE, \quad (1)$$

$$\Delta T = -\frac{T}{\rho} \int_{E_1}^{E_2} \frac{1}{C} \left( \frac{\partial P}{\partial T} \right)_E dE, \quad (2)$$

where  $\Delta T$  is the adiabatic temperature change and  $\Delta S$  is the isothermal entropy change,  $T$  is the measured temperature,  $E_1$  and  $E_2$  are, respectively, the initial and ultimate electric field,

$P$  is the electric field-induced polarization,  $\rho$  is the density and  $C$  is the heat capacity per mass. According to the above expressions, the highest electrocaloric response is usually obtained in the phase-transition temperature due to the most rapid polarization change near the phase transition.<sup>13</sup>

The ferroelectric bulk ceramics can be easily prepared and can achieve high refrigeration volume, thus attracting the main attention in recent studies. Barium titanate (BaTiO<sub>3</sub>, BT)-based ceramics are lead-free ferroelectric materials, which possess a high polarization and a relatively low Curie temperature ( $T_C$ ), thus the enhanced electrocaloric properties can be easily achieved after shifting the  $T_C$  to room temperature through chemical modification, such as A- or B-site ions doping and defects regulation.<sup>14–21</sup> Therefore, BT-based ferroelectric ceramics is one of the most studied electrocaloric materials currently. Based on Eqs. (1) and (2), the electrocaloric properties ( $\Delta T$  and  $\Delta S$ ) can be calculated according to a series of ferroelectric measurements to obtain the polarization change rate,  $(\partial P/\partial T)_E$ . That is, the ferroelectric performance and its evolution show a significant influence on the electrocaloric property. On the other hand, the measurement frequency of the driving electric field can affect the ferroelectric performance due to the different behavior of polarization rotation and domain switching at different frequencies.<sup>22</sup> Therefore, different behaviors of ferroelectric

performance at different frequencies mean that different electrocaloric responses will be observed at different excited frequencies. Nowadays, the electrocaloric properties can be acquired by the direct method based on self-made and non-standardized instruments or by the indirect method based on Maxwell relations [Eqs. (1) and (2)].<sup>23</sup> Thus, before the development of standardized electrocaloric measuring instruments and the actual applications of electrocaloric cooling technology, the frequency dependence of electrocaloric properties based on Maxwell relations needs to be investigated.

In this work, the frequency-dependent ferroelectric and electrocaloric properties near/above room temperature are studied based on Maxwell relations.  $Zr^{4+}$  is a typical ion that can effectively shift the low-temperature phase transitions of BT ceramic to high temperature, meanwhile  $T_C$  will be shifted to low temperature. Less  $Zr^{4+}$  doping cannot shift low-temperature phase transitions to surpass room temperature, while more  $Zr^{4+}$  doping will lead to the merging phenomenon between different phase transitions. Therefore, 8%  $Zr^{4+}$ -doped BT-based ceramic is selected as the paradigm since the general phase structures and phase transitions of BT ceramic can be clearly observed in this composition above room temperature.<sup>14</sup> Therefore, the frequency dependence of ferroelectric and electrocaloric properties can be investigated and compared among different phase structures. A series of ferroelectric hysteresis loops are measured at different frequencies of 0.1–10 Hz, and then the evolution behavior and frequency dependence of ferroelectric parameters and electrocaloric performances are analyzed, and the differences of these frequency dependences under different electric fields are also compared. It is found that a higher electrocaloric property is present in low frequency, and the electrocaloric properties and ferroelectric polarization gradually decrease with increasing frequency due to more difficult polarization rotation and domain switching under high frequency, especially in the phase-structure state with stable ferroelectric phases.

## 2. Experimental Section

The  $BaCO_3$  (0.99),  $ZrO_2$  (0.99) and  $TiO_2$  (0.98) were purchased (Sinopharm Chemical Reagent Co., Ltd) and used as raw materials to prepare  $Ba(Ti_{0.92}Zr_{0.08})O_3$  ceramic via the conventional solid-state method. The mixed raw materials were calcined at  $1240^\circ C$  for 3 h and then were pressed into disks of 1 mm thickness and 10 mm diameter under  $\sim 100$  MPa using the binder of 8 wt.% polyvinyl alcohol (PVA). After burning out PVA at  $800^\circ C$ , the green pellets were sintered at  $1360^\circ C$  for 3 h. The sintered ceramics were coated with silver paint on the whole upper and bottom surfaces and kept at  $550^\circ C$  (10 min) to obtain the silver electrodes.

The phase structure was analyzed using the temperature-dependent dielectric constant ( $\epsilon_r-T$ ) and dielectric loss ( $\tan \delta-T$ ) curves via a dielectric meter (TH2816A, China) and X-ray diffraction (XRD) analysis with Cu  $K\alpha$  radiation

(Rigaku Ultima III, Rigaku Corporation, Japan). The  $\epsilon_r-T$  and  $\tan \delta-T$  curves were measured from  $-50$  to  $150^\circ C$  and from 100 Hz to 100 kHz using the silver-plated ceramics. The heat capacity was measured by a differential scanning calorimeter (DSC214, Netzsch). Temperature, frequency and electric field dependence ferroelectric hysteresis ( $P-E$ ) loops were measured via a ferroelectric tester (TF Analyzer 2000E, aixACCT Systems GmbH, Germany). The  $P-E$  loops were measured from room temperature to  $140^\circ C$  at 0.1–10 Hz and 2.5–20 kV/cm using the silver-plated ceramics. The electrocaloric properties were calculated based on the measured ferroelectric results and Maxwell relations.

## 3. Results and Discussion

Figure 1(a) shows the  $\epsilon_r-T$  and  $\tan \delta-T$  curves at different frequencies of  $Ba(Ti_{0.92}Zr_{0.08})O_3$  ceramic, displaying the room-temperature phase structure and the transition of phase structure when the temperature is elevated. The phase transition temperatures from ferroelectric rhombohedral ( $R$ ) phase to orthorhombic ( $O$ ) phase ( $T_{R-O}$ ), subsequently to tetragonal ( $T$ ) phase ( $T_{O-T}$ ), and finally to paraelectric cubic ( $C$ ) phase ( $T_C$ ) are found to be  $\sim 44^\circ C$ ,  $\sim 68^\circ C$  and  $\sim 99^\circ C$ . Compared to pure BT ceramic,<sup>24</sup> these three phase-transition temperatures have been shifted toward above the room temperature and get closer to each other after introducing 8%

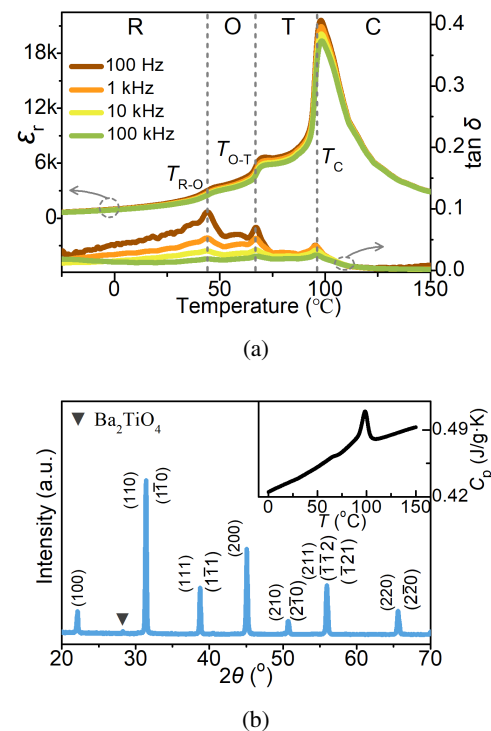


Fig. 1. (a)  $\epsilon_r-T$  and  $\tan \delta-T$  curves of  $Ba(Ti_{0.92}Zr_{0.08})O_3$  ceramic under different frequencies. (b) XRD pattern of  $Ba(Ti_{0.92}Zr_{0.08})O_3$  ceramic, and the inset shows the heat capacity ( $C_p$ ) curve.

Zr<sup>4+</sup> into BT ceramic. Therefore, the general phase structures and phase transitions of BT ceramic are present in this ceramic over room temperature. Figure 1(b) shows the room-temperature XRD pattern and heat capacity ( $C_p$ ) curve of Ba(Ti<sub>0.92</sub>Zr<sub>0.08</sub>)O<sub>3</sub> ceramic. Similar phase transitions can be observed in the heat capacity curve. The perovskite structure is present in this ceramic, indicating the introduced Zr<sup>4+</sup> is well-doped into the BT matrix. It can be observed that a little secondary phase (Ba<sub>2</sub>TiO<sub>4</sub>) is found in the XRD pattern, which should result from the regional heterogeneous reaction within ceramic in the preparation process of the conventional solid-state method.<sup>15</sup> In addition, the density of this ceramic is about 5.75 g/cm<sup>2</sup>.

To investigate the frequency-dependent ferroelectric and electrocaloric properties in BT-based ceramics, the ferroelectric  $P$ - $E$  loops are measured under different electric fields, temperatures and frequencies. The measuring electric field of the triangular waveform is employed, then the different triangular waveforms with different electric fields and loading periods (frequencies) are set to obtain various  $P$ - $E$  loops,<sup>22</sup> as shown in Fig. 2(a). Figure 2(b) displays the room-temperature  $P$ - $E$  loops measured from 2.5 to 20 kV/cm. It can be seen that the  $P$ - $E$  loop gradually becomes a saturation shape when an electric field is elevated, indicating that the domain switching becomes sufficient under a high electric field. Figure 2(c) presents the evolution of maximum polarization ( $P_{\max}$ ), remnant polarization ( $P_r$ ) and coercive field ( $E_c$ ) at room temperature. By raising the electric field, these three ferroelectric parameters increase fast in the low-electric field range and then display a slow increasing rate. Specifically,  $P_{\max}$  quickly increases from 11.90 to 18.85  $\mu\text{C}/\text{cm}^2$  when the electric field is elevated from 2.5 to 7.5 kV/cm, and then slowly increases to 21.72  $\mu\text{C}/\text{cm}^2$  while raising the electric field to 20 kV/cm. In this process,  $P_r$  quickly increases from 9.61 to 13.86, then slowly increases to 15.30  $\mu\text{C}/\text{cm}^2$  and  $E_c$  quickly increases from 1.20  $\pm$  0.08 to 1.71  $\pm$  0.18 then slowly increases to 2.02  $\pm$  0.25 kV/cm.

Figures 3(a) and 3(b) show the room-temperature  $P$ - $E$  loops measured from 0.1 to 10 Hz under a low electric field of

2.5 kV/cm and a relatively high electric field of 10 kV/cm, respectively. It can be seen that the measuring frequency shows an obvious effect on the ferroelectric  $P$ - $E$  loops no matter whether the driving electric field is low or high. The relatively square  $P$ - $E$  loops are observed at a low frequency. With increasing frequency, the  $P$ - $E$  loops gradually become compressed, with the reduction in  $P_{\max}$  and  $P_r$  and the increase in  $E_c$ . This result indicates that the ferroelectric domain of BT-based ceramics can be easily switched under a low-frequency electric field driving. When the frequency of the driving electric field is elevated, the domain switching will become difficult and thus the obtained macroscopic polarization will decrease.<sup>25,26</sup> For example, as shown in Fig. 3(c), when the frequency of driving electric field (10 kV/cm) increases from 0.1 to 10 Hz,  $P_{\max}$  decreases from 19.98 to 19.03  $\mu\text{C}/\text{cm}^2$  for Ba(Ti<sub>0.92</sub>Zr<sub>0.08</sub>)O<sub>3</sub> ceramic,  $P_r$  decreases from 14.53 to 12.90  $\mu\text{C}/\text{cm}^2$  and  $E_c$  increases from 1.47  $\pm$  0.14 to 2.01  $\pm$  0.23 kV/cm. On the other hand, the change rate of  $P_{\max}$ ,  $P_r$  and  $E_c$  is different under different electric fields. As shown in Fig. 3(d), the decrease rate of  $P_{\max}$  and  $P_r$  under a low-electric field (2.5 kV/cm) is much faster than that under a high-electric field (10 kV/cm), while the increase rate of  $E_c$  under a low-electric field is much slower than that under a high-electric field. This phenomenon indicates that the frequency influence on  $P_{\max}$  and  $P_r$  is obvious under a low-electric field, while this influence can be weakened by increasing the driving electric field. Besides, the frequency influence on  $E_c$  and the difficulty of domain switching is small under a low-electric field, while this influence becomes more obvious if the driving electric field is elevated. In addition, when the frequency is below 1 Hz, the change rate of  $P_{\max}$ ,  $P_r$  and  $E_c$  is quite large, while the change rate becomes small when the frequency is over 1 Hz. This result demonstrates that the frequency change in a low-frequency range (< 1 Hz) shows a significant influence on domain switching and ferroelectric properties of BT-based ceramics, while the frequency dependence will become small in the high-frequency range.

Figures 4(a)–4(c) display the  $P$ - $E$  loops as a function of temperature under 5 kV/cm and different frequencies of

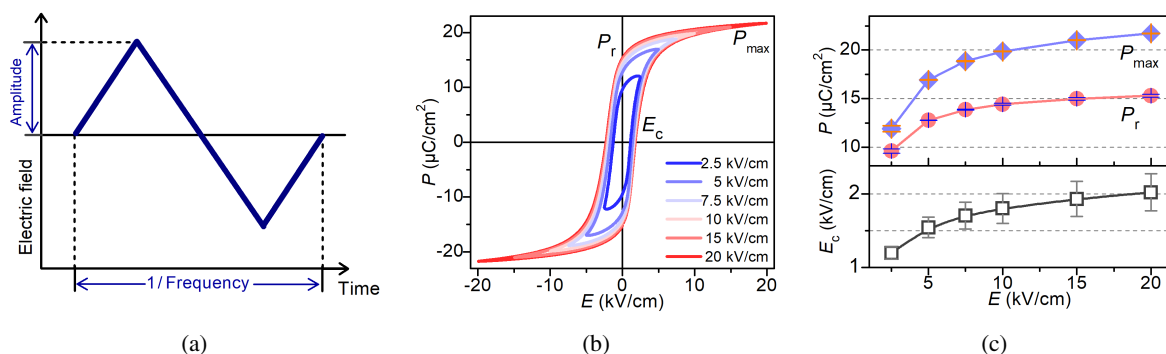


Fig. 2. (a) Schematic showing the triangular waveform of applied electric field for ferroelectric  $P$ - $E$  loops measurement. (b) Electric field dependence of room-temperature  $P$ - $E$  loops for Ba(Ti<sub>0.92</sub>Zr<sub>0.08</sub>)O<sub>3</sub> ceramic from 2.5 to 20 kV/cm. (c) Evolution of  $P_{\max}$ ,  $P_r$  and  $E_c$  for Ba(Ti<sub>0.92</sub>Zr<sub>0.08</sub>)O<sub>3</sub> ceramic with increasing electric field.

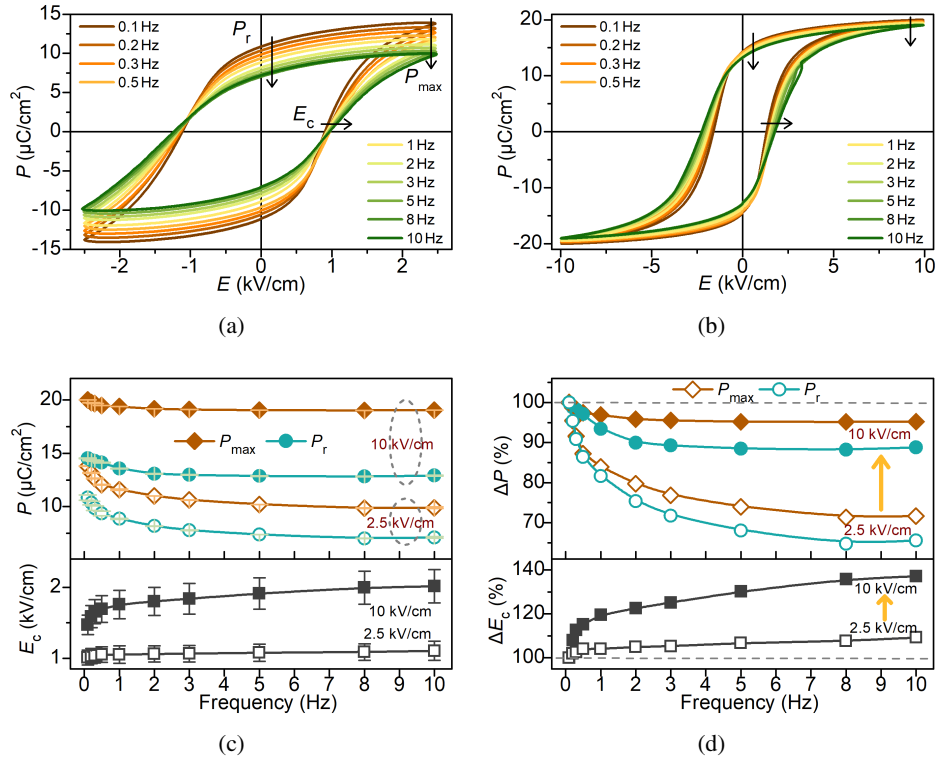


Fig. 3. Frequency dependence of  $P$ - $E$  loops for  $\text{Ba}(\text{Ti}_{0.92}\text{Zr}_{0.08})\text{O}_3$  ceramic measured from 0.1 to 10 Hz under (a) 2.5 kV/cm and (b) 10 kV/cm. Evolution of (c)  $P_{\max}$ ,  $P_r$  and  $E_c$  with increasing measuring frequencies. (d) Variation rate of  $P_{\max}$ ,  $P_r$  and  $E_c$  with increasing measuring frequencies from 0.1 to 10 Hz.

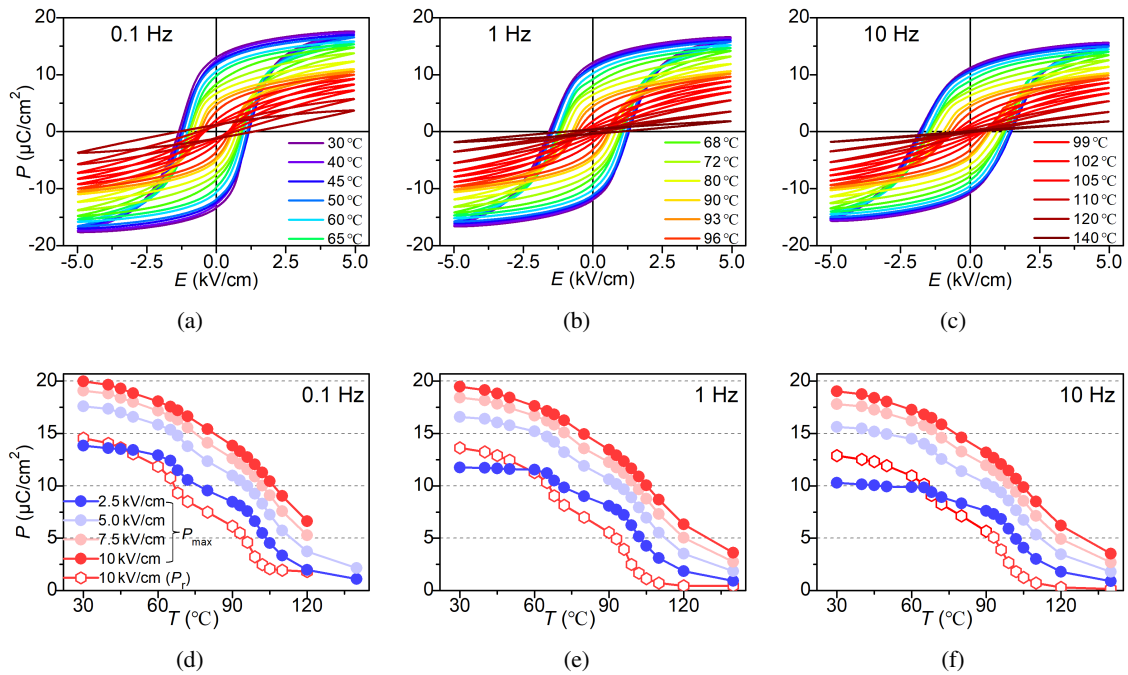


Fig. 4. Temperature dependence of  $P$ - $E$  loops (5 kV/cm) for  $\text{Ba}(\text{Ti}_{0.92}\text{Zr}_{0.08})\text{O}_3$  ceramic measured at (a) 0.1 Hz, (b) 1 Hz and (c) 10 Hz. Temperature dependence of electric field-induced polarization for  $\text{Ba}(\text{Ti}_{0.92}\text{Zr}_{0.08})\text{O}_3$  ceramic measured at (d) 0.1 Hz, (e) 1 Hz and (f) 10 Hz.

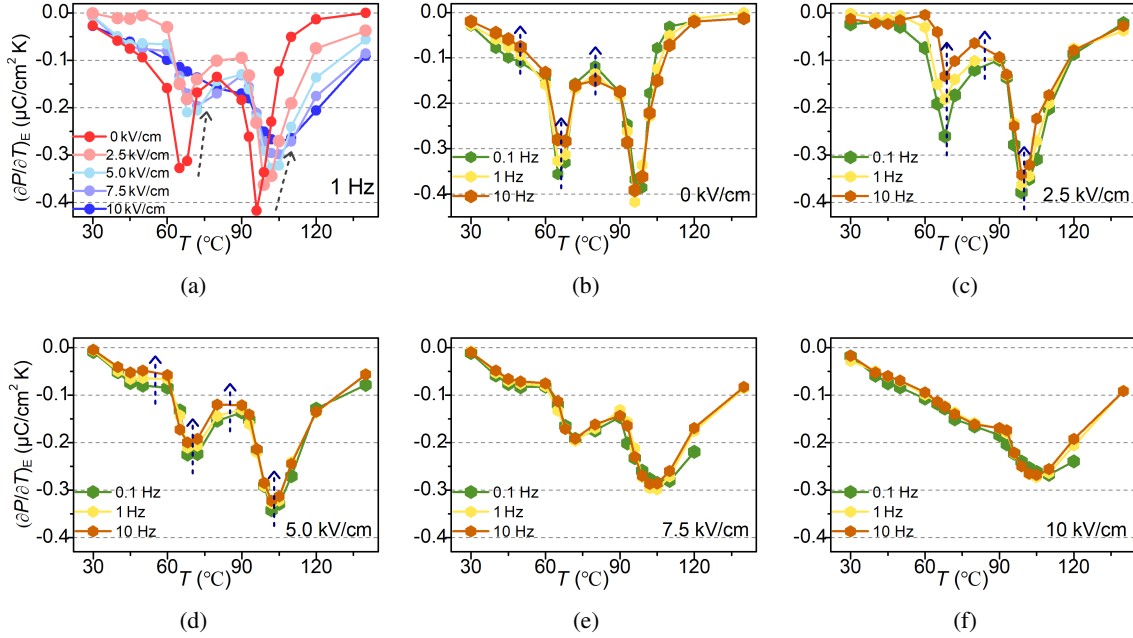


Fig. 5. (a) Electric field dependence of polarization variation rate against temperature  $(\partial P/\partial T)_E$  (1 Hz) for  $\text{Ba}(\text{Ti}_{0.92}\text{Zr}_{0.08})\text{O}_3$  ceramic at different temperatures. (b)–(f) Evolution of temperature-dependent  $(\partial P/\partial T)_E$  among 0.1, 1 and 10 Hz for  $\text{Ba}(\text{Ti}_{0.92}\text{Zr}_{0.08})\text{O}_3$  ceramic under different electric fields.

0.1, 1 and 10 Hz for  $\text{Ba}(\text{Ti}_{0.92}\text{Zr}_{0.08})\text{O}_3$  ceramic. The low-temperature  $P$ – $E$  loop shows a square shape with high  $P_{\max}$  and  $P_r$  and a large  $E_c$ . No matter if the frequency is low or high, the  $P$ – $E$  loops all become slim with increasing temperature, showing a decreased  $P_{\max}$ ,  $P_r$  and  $E_c$ . The evolution of  $P_{\max}$  (2.5–10 kV/cm) and  $P_r$  (10 kV/cm) from 30°C to 140°C is present in Figs. 4(d) and 4(e). It can be seen that the  $P_{\max}$  and  $P_r$  at 0.1 Hz are higher than the  $P_{\max}$  and  $P_r$  at 1 Hz and 10 Hz for all the temperatures. All the  $P_{\max}$  and  $P_r$  present a much quicker decrease rate at the phase-transition temperature of  $T_{O-T}$  and  $T_C$ , and the decrease rate at 0.1 Hz is also faster than the decrease rate at 1 Hz and 10 Hz. For example, under 5 kV/cm and 0.1 Hz,  $P_{\max}$  first decreases from 17.59 to 15.36  $\mu\text{C}/\text{cm}^2$  when temperature is elevated from 30°C to 65°C, then fast decreases from 14.80 to 10.98  $\mu\text{C}/\text{cm}^2$  when temperature is elevated from 68 ( $T_{O-T}$ ) to 90°C (closing to  $T_C$  phase transition peak), and finally decrease more quickly from 10.54 to 2.14  $\mu\text{C}/\text{cm}^2$  when the temperature gets through  $T_C$  peak and is elevated to 140°C. Similarly, for 1 Hz, the evolution of  $P_{\max}$  is from 16.59 to 14.70, then from 14.18 to 10.61, and finally from 10.18 to 1.85  $\mu\text{C}/\text{cm}^2$ . For 10 Hz, the evolution of  $P_{\max}$  is from 15.63 to 14.03, then from 13.45 to 10.25, and finally from 9.86 to 1.81  $\mu\text{C}/\text{cm}^2$ . However, the decreased tendency of  $P_{\max}$  among phase transition temperature gradually becomes weak under a high electric field, which should result from the electric field-induced polarization under a high electric field.<sup>27</sup>

The electrocaloric effect is directly dependent on the change rate of polarization with temperature, that is the  $(\partial P/\partial T)_E$ . Based on the results in Figs. 4(d) and 4(e),

the evolution  $(\partial P/\partial T)_E$  as a function of electric field, temperature and frequency can be obtained, as shown in Fig. 5. Figure 5(a) gives the temperature-dependent  $(\partial P/\partial T)_E$  of  $\text{Ba}(\text{Ti}_{0.92}\text{Zr}_{0.08})\text{O}_3$  ceramic under different electric fields at 1 Hz. It can be seen that all the  $(\partial P/\partial T)_E$  are negative values because of the depolarization behavior with temperature increasing for BT-based ceramics. The peak  $(\partial P/\partial T)_E$  is obtained near the phase-transition temperature of  $T_{O-T}$  and  $T_C$  due to the quick polarization change around phase transitions. In addition,  $(\partial P/\partial T)_E$  becomes small and slightly shifts to high temperature with increasing electric field. This is because the depolarization process around the phase-transition region will be retarded due to the polarization compensation derived from electric field-induced polarization under a high electric field.<sup>27,28</sup> Figures 5(b)–5(f) show the comparison of  $(\partial P/\partial T)_E$  at different frequencies under different electric fields. It can be seen that  $(\partial P/\partial T)_E$  shows the obvious frequency dependence, especially among the low-temperature region (below  $T_C$  peak). In the low-temperature single-phase and phase-transition regions, the absolute value of  $(\partial P/\partial T)_E$  all decreases with the frequency improvement. However, this frequency dependence becomes small in the relatively high-temperature region, except at the  $T_C$  point where the  $(\partial P/\partial T)_E$  also displays a little frequency dependence. This phenomenon indicates that the faster polarization change can be achieved at a low frequency, while the high frequency shows a negative effect on the polarization change for the low-temperature region with stable ferroelectric structure. In addition, this frequency dependence gradually becomes weak with increasing electric field, indicating that

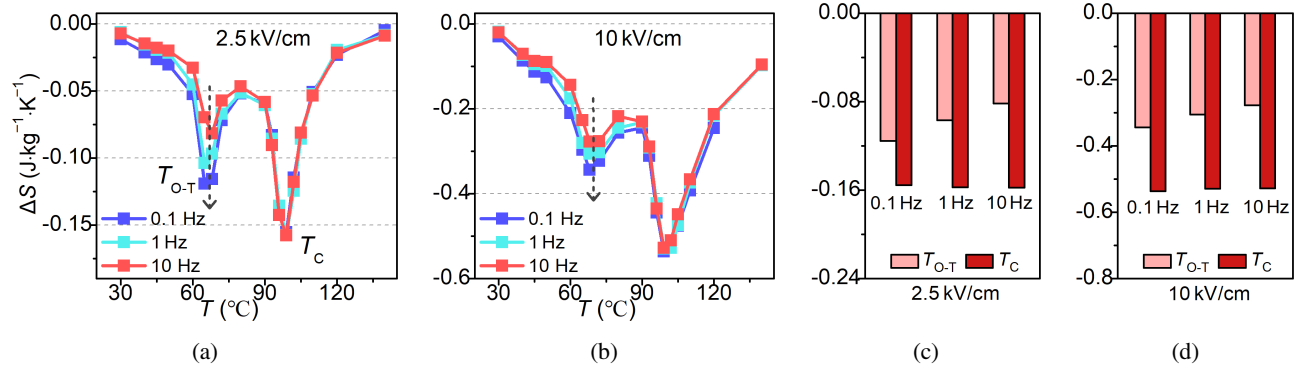


Fig. 6. Evolution of  $\Delta S$  among 0.1, 1, and 10 Hz under (a) a low-electric field of 2.5 kV/cm and (b) a relatively high-electric field of 10 kV/cm. Comparison of  $\Delta S$  at the temperature point of  $T_{O-T}$  and  $T_C$  among 0.1, 1 and 10 Hz under (c) 2.5 and (d) 10 kV/cm.

the high-electric field can weaken the frequency effect on the polarization change rate.

According to the Maxwell relations [Eqs. (1) and (2)], the electrocaloric isothermal entropy change ( $\Delta S$ ) and adiabatic temperature change ( $\Delta T$ ) can be obtained. Figures 6(a) and 6(b) compare  $\Delta S$  among 0.1, 1 and 10 Hz under a low or high-electric field. It is clear that all the  $\Delta S$  are negative values. This is because the disorder polarization vectors of ferroelectrics become ordered after applying the electric field.<sup>10</sup> The peak  $\Delta S$  value is obtained near the  $T_C$ , where the most rapid polarization change contributes to the highest electrocaloric response. Importantly,  $\Delta S$  is similar around  $T_C$  peak and above  $T_C$ , showing tiny frequency dependence that  $\Delta S$  slightly decreases with rising frequency. However, the obvious frequency dependence is observed below the  $T_C$  peak, especially in the  $T_{O-T}$  phase-transition region, and this frequency dependence is more obvious under a low-electric field. According to the above results, the frequency dependence of  $\Delta S$  should result from the frequency-dependent domain switching with a relatively stable ferroelectric structure in the low-temperature region.<sup>29</sup> Especially, the significant frequency dependence of  $\Delta S$  is observed at  $T_{O-T}$  due to the relatively high isothermal entropy change displays near  $T_{O-T}$ . As shown in Figs. 6(c) and 6(d), the  $\Delta S$  values at  $T_C$  show a tiny decrease with increasing frequency under a low or a high-electric field. However, the  $\Delta S$  values at  $T_{O-T}$  show an obvious decrease with increasing frequency no matter whether the electric field is low or high. With increasing frequency from 0.1 to 1 then to 10 Hz,  $\Delta S$  decreases from 0.116 to 0.097 then to 0.082 J/(kg·K) under 2.5 kV/cm and  $\Delta S$  decreases from 0.344 to 0.306 then to 0.277 J/(kg·K) under 10 kV/cm.

Figure 7(a) shows the  $\Delta T$  evolution with changing temperature and electric field at 1 Hz for Ba(Ti<sub>0.92</sub>Zr<sub>0.08</sub>)O<sub>3</sub> ceramic. A small  $\Delta T$  displays in the single-phase region under a low-electric field, while the increase in  $\Delta T$  is present in the phase-transition region ( $T_{O-T}$  and  $T_C$ ) with an increasing electric field. The maximum  $\Delta T$  is obtained near the  $T_C$ , which increases from 0.38 to 0.61, then to 0.83 and 1.02 K when the electric field is elevated from 10 to 20, then to 30

and 40 kV/cm, respectively. On the other hand, electrocaloric  $\Delta T$  also shows frequency dependence in the low-temperature range similar to  $\Delta S$ . As shown in Figs. 7(b)–7(e),  $\Delta T$  is similar around  $T_C$  peak and above  $T_C$ , displaying the weak frequency dependence. Nevertheless,  $\Delta T$  below the  $T_C$  peak presents the obvious frequency dependence, especially around  $T_{O-T}$  where the metastable phase structure and relatively high electrocaloric properties are shown, and the more obvious frequency dependence is also observed under a low-electric field. The significant frequency dependence of domain switching in the stable ferroelectric region should also contribute to this phenomenon.<sup>29</sup> Figure 7(f) shows the comparison of maximum  $\Delta T$  values (10 kV/cm) at  $T_{O-T}$  and  $T_C$  with increasing frequency from 0.1 to 1 then to 10 Hz. The maximum  $\Delta T$  at  $T_C$  shows a small change from 0.390 to 0.383 and then to 0.377 K. In comparison, the maximum  $\Delta T$  at  $T_{O-T}$  shows an obvious reduction from 0.254 to 0.225 and then to 0.204 K, indicating that the frequency exhibits a significant influence on electrocaloric properties, and a higher  $\Delta T$  can be obtained under a low frequency, especially in the temperature region below  $T_C$ .

The electrocaloric strength  $\Delta T/\Delta E$  is another important electrocaloric parameter, which represents the intensity of electrocaloric response under a unit electric field. Figures 8(a)–8(c) show the evolution of  $\Delta T/\Delta E$  with temperature and electric field variation at 0.1, 1 and 10 Hz. An enhanced  $\Delta T/\Delta E$  is also obtained in the phase-transition region ( $T_{O-T}$  and  $T_C$ ), while the maximum  $\Delta T/\Delta E$  is achieved under a low-electric field and  $\Delta T/\Delta E$  becomes small when the electric field is elected. This change tendency is opposite to the variation of  $\Delta T$ .<sup>30</sup> This phenomenon indicates that the highest unit electrocaloric response is present at a low-electric field, which results from the most entropy change and fastest polarization change rate in the beginning process of domain switching by applying an electric field (Fig. 5). However, this electric field dependence becomes small after increasing the frequency. On the other hand,  $\Delta T/\Delta E$  still shows the obvious frequency dependence in the low-temperature range and a tiny frequency dependence at  $T_C$ , and this frequency dependence gradually becomes small

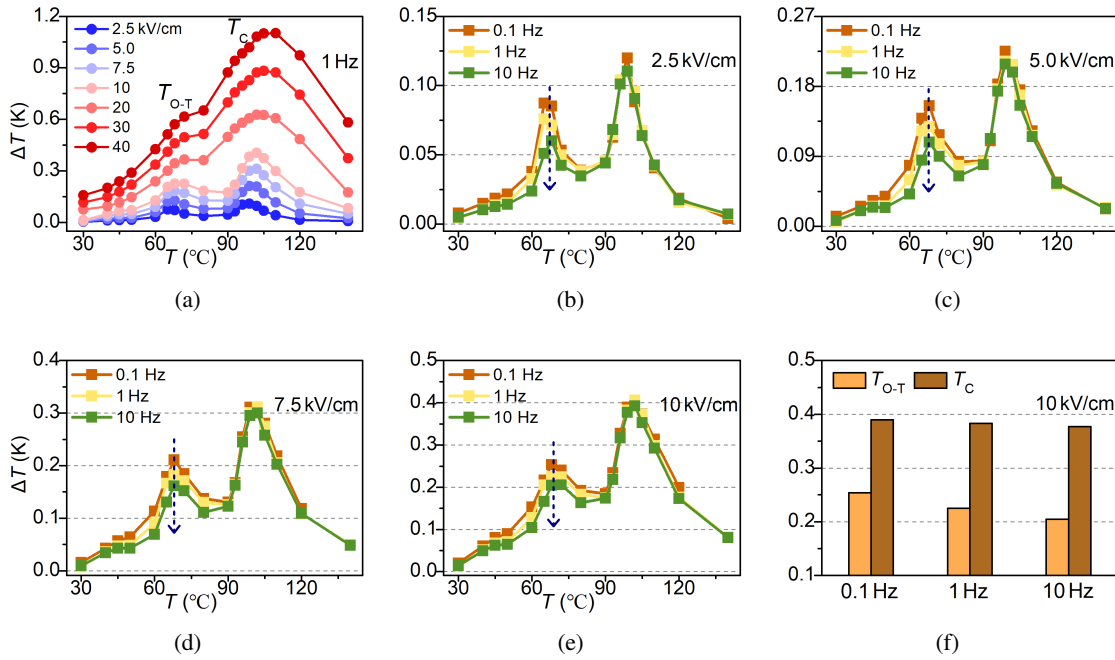


Fig. 7. (a) Electric field dependence of electrocaloric  $\Delta T$  (1 Hz) based on Maxwell relations for  $\text{Ba}(\text{Ti}_{0.92}\text{Zr}_{0.08})\text{O}_3$  ceramic at different temperatures. (b)–(e) Evolution of  $\Delta T$  among 0.1, 1 and 10 Hz under different electric fields. (f) Comparison of  $\Delta T$  at the temperature point of  $T_{O-T}$  and  $T_C$  among 0.1, 1 and 10 Hz under 10 kV/cm.

with increasing electric field, as shown in Figs. 8(d) and 8(e). Figure 8(f) exhibits the comparison of  $\Delta T/\Delta E$  (2.5 kV/cm) at  $T_{O-T}$  and  $T_C$  with increasing frequency from 0.1 to 1 then to 10 Hz.  $\Delta T/\Delta E$  at  $T_C$  shows a slight variation around

0.045–0.046  $\text{K}\cdot\text{mm}/\text{kV}$ , while  $\Delta T/\Delta E$  at  $T_{O-T}$  displays a decreasing tendency from 0.034 to 0.029 than to 0.024  $\text{K}\cdot\text{mm}/\text{kV}$ , indicating that a higher  $\Delta T/\Delta E$  can be obtained under a low frequency.

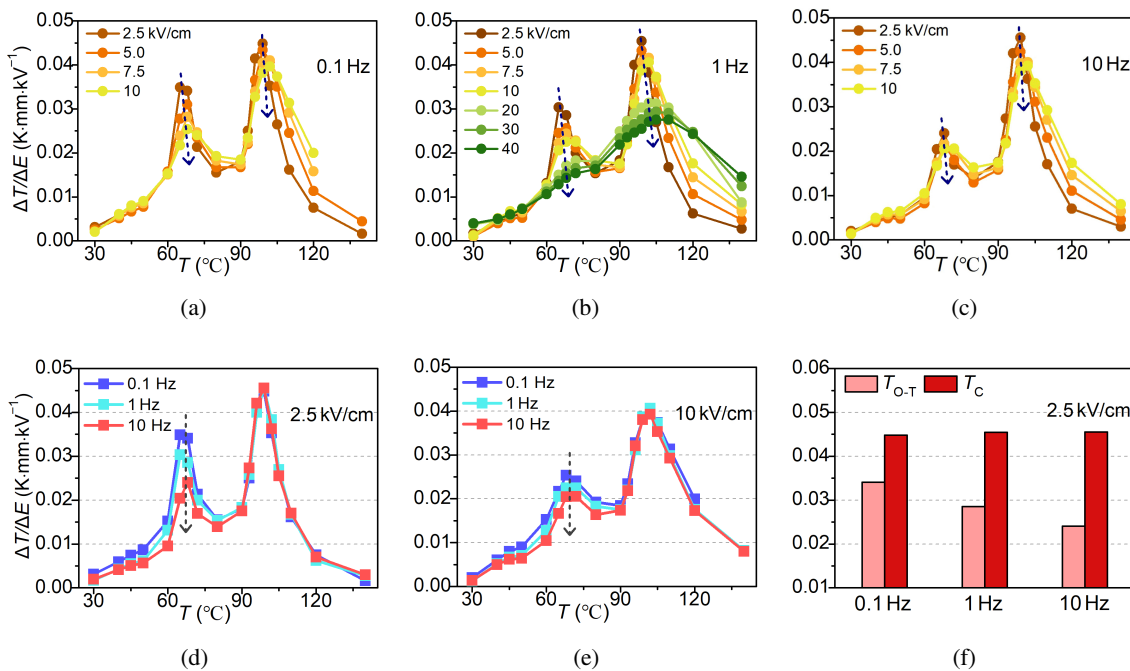


Fig. 8. Electric field and temperature dependence of electrocaloric strength  $\Delta T/\Delta E$  for  $\text{Ba}(\text{Ti}_{0.92}\text{Zr}_{0.08})\text{O}_3$  ceramic at (a) 0.1, (b) 1 and (c) 10 Hz. (d) and (e) Evolution of  $\Delta T/\Delta E$  among 0.1, 1 and 10 Hz under a low and a high electric field. (f) Comparison of  $\Delta T/\Delta E$  at the temperature point of  $T_{O-T}$  and  $T_C$  among 0.1, 1 and 10 Hz under 2.5 kV/cm.

#### 4. Conclusions

In this study, the frequency dependence of electrocaloric properties is systemically investigated based on the Maxwell relations and a paradigmatic BT-based ferroelectric ceramic. The electrocaloric parameters of  $\Delta S$ ,  $\Delta T$  and  $\Delta T/\Delta E$  are all found to show obvious frequency dependence, especially in the temperature range below the  $T_C$  peak. This is because the measuring frequency shows a significant influence on the domain switching and ferroelectric performance. However, the frequency dependence of electrocaloric properties will become small when increasing the electric field and around  $T_C$  peak and above  $T_C$ . On the other hand, increasing the measuring frequency can weaken the electric field dependence of electrocaloric strength. This work gives significant guidance for further deep study of electrocaloric properties and the applications of electrocaloric cooling technology.

#### Acknowledgments

The authors appreciate the support of the National Natural Science Foundation of China (Nos. 12204104, 12104093, 52102126 and 52072075), the Natural Science Foundation of Fujian Province (Nos. 2021J05122, 2021J05123, 2022J01087, 2022J01552 and 2023J01259) and Qishan Scholar Financial Support from Fuzhou University (No. GXRC-20099). Wanting Shu and Hong Li contributed equally to this work.

#### ORCID

Yanli Huang  <https://orcid.org/0000-0002-2637-0996>  
 Cong Lin  <https://orcid.org/0000-0003-4926-2776>  
 Xiao Wu  <https://orcid.org/0000-0002-2173-1086>  
 Min Gao  <https://orcid.org/0000-0001-8063-3753>  
 Tengfei Lin  <https://orcid.org/0000-0001-7428-9829>  
 Chunlin Zhao  <https://orcid.org/0000-0003-1333-1864>

#### References

- M. Valant, Electrocaloric materials for future solid-state refrigeration technologies, *Prog. Mater. Sci.* **57**, 980 (2012).
- J. Shi, D. Han, Z. Li, L. Yang, S.-G. Lu, Z. Zhong, J. Chen, Q. Zhang and X. Qian, Electrocaloric cooling materials and devices for zero-global-warming-potential, high-efficiency refrigeration, *Joule* **3**, 1200 (2019).
- Y. Ying, D. Hongliang, Y. Zetian, J. Li and Q. Shaobo, Electrocaloric effect of lead-free bulk ceramics: Current status and challenges, *J. Inorg. Mater.* **35**, 633 (2020).
- X. Qian, D. Han, L. Zheng, J. Chen, M. Tyagi, Q. Li, F. Du, S. Zheng, X. Huang and S. Zhang, High-entropy polymer produces a giant electrocaloric effect at low fields, *Nature* **600**, 664 (2021).
- H. Tao, J. Yin, C. Zhao, B. Wu, L. Zhao, J. Ma and J. Wu, Large electrocaloric effect under electric field behavior in potassium sodium niobate ceramics with incompletely overlapped phase boundaries, *J. Mater. Chem. A* **10**, 5262 (2022).
- R. Yin, J. Li, X. Su, S. Qin, C. Yu, Y. Hou, C. Liu, Y. Su, L. Qiao and T. Lookman, Emergent enhanced electrocaloric effect within wide temperature span in laminated composite ceramics, *Adv. Funct. Mater.* **32**, 2108182 (2022).
- Y. Zhou, R. Xiong, P. Wang, X. W. P. Envelope, B. Sa, C. Lin, M. Gao, T. Lin and C. Z. P. Envelope, Strain and illumination triggered regulations of up-conversion luminescence in Er-doped  $\text{Bi}_{0.5}\text{Na}_{0.5}\text{TiO}_3/\text{BaTiO}_3/\text{Mica}$  flexible multifunctional thin films, *J. Materiomics* **8**, 586 (2022).
- G. Li, C. Shi, K. Zhu, G. Ge, F. Yan, J. Lin, Y. Shi, B. Shen and J. Zhai, Achieving synergistic electromechanical and electrocaloric responses by local structural evolution in lead-free BNT-based relaxor ferroelectrics, *Chem. Eng. J.* **431**, 133386 (2022).
- B. Nair, T. Usui, S. Crossley, S. Kurdi, G. Guzmán-Verri, X. Moya, S. Hirose and N. Mathur, Large electrocaloric effects in oxide multilayer capacitors over a wide temperature range, *Nature* **575**, 468 (2019).
- J. Scott, Electrocaloric materials, *Annu. Rev. Mater. Res.* **41**, 229 (2011).
- T. Correia and Q. Zhang, *Electrocaloric Materials: New Generation of Coolers* (Springer Berlin, Heidelberg, 2014).
- M. Ožbolt, A. Kitanovski, J. Tušek and A. Poredoš, Electrocaloric refrigeration: Thermodynamics, state of the art and future perspectives, *Int. J. Refrig.* **40**, 174 (2014).
- X. Moya, S. Kar-Narayan and N. D. Mathur, Caloric materials near ferroic phase transitions, *Nat. Mater.* **13**, 439 (2014).
- C. Zhao, Y. Huang and J. Wu, Multifunctional barium titanate ceramics via chemical modification tuning phase structure, *Info-Mat* **2**, 1163 (2020).
- H. Li, B. Wu, C. Lin, X. Wu, T. Lin, M. Gao, H. Tao, W. Wu and C. Zhao, Microscopic origin and relevant grain size effect of discontinuous grain growth in  $\text{BaTiO}_3$ -based ferroelectric ceramics, *J. Mater. Sci. Technol.* **164**, 119 (2023).
- S. Zhong, C. Zhao, B. Li, L. Zhang, Y. Huang and J. Wu, Tuning the electrocaloric effect by tailoring phase fraction in  $\text{BaTiO}_3$ -based ferroelectrics, *J. Eur. Ceram. Soc.* **42**, 5172 (2022).
- X. Wei, C. Zhao, T. Zheng, X. Lv, L. Zhang, B. Li and J. Wu, Understanding the enhanced electrocaloric effect in  $\text{BaTiO}_3$ -based ferroelectrics at critical state, *Acta Mater.* **227**, 117735 (2022).
- Y. Huang, C. Zhao, B. Wu and X. Zhang, Grain size effects and structure origin in high-performance  $\text{BaTiO}_3$ -based piezoceramics with large grains, *J. Eur. Ceram. Soc.* **42**, 2764 (2022).
- C. Zhao, Y. Huang, X. Wu, M. Gao, T. Lin and C. Lin, Evolution behavior of electrocaloric effect in  $\text{BaTiO}_3$ -based ceramics with different phase structures and phase transitions, *J. Am. Ceram. Soc.* **107**, 195 (2024).
- X. Niu, X. Jian, X. Chen, H. Li, W. Liang, Y. Yao, T. Tao, B. Liang and S. Lu, Enhanced electrocaloric effect at room temperature in  $\text{Mn}^{2+}$  doped leadfree ( $\text{BaSr}$ ) $\text{TiO}_3$  ceramics via a direct measurement, *J. Adv. Ceram.* **10**, 482 (2021).
- C. Zhang, Z. Dou, S. Zeng, K. Li, F. Zeng, W. Xiao, S. Qiu, G. Fan, S. Jiang, W. Luo, Q. Fu and G. Zhang, Substantially enhanced electrocaloric effect in  $\text{Ba}(\text{Zr}_{0.2}\text{Ti}_{0.8})\text{O}_3$  lead-free ferroelectric ceramics via lattice stress engineering, *ACS Appl. Mater. Interfaces* **15**, 18065 (2023).
- L. Jin, F. Li and S. Zhang, Decoding the fingerprint of ferroelectric loops: Comprehension of the material properties and structures, *J. Am. Ceram. Soc.* **97**, 1 (2014).

- <sup>23</sup>Y. Liu, J. F. Scott and B. Dkhil, Direct and indirect measurements on electrocaloric effect: Recent developments and perspectives, *Appl. Phys. Rev.* **3**, 031102 (2016).
- <sup>24</sup>C. Zhao, T. He, C. Lin, X. Wu, T. Lin, M. Gao, H. Tao, W. Wu and B. Wu, Comparison of electric field-dependent property in BaTiO<sub>3</sub>-based piezoceramics between single and coexisting phases, *J. Am. Ceram. Soc.* **106**, 5381 (2023).
- <sup>25</sup>X. Lv, T. Zheng, C. Zhao, J. Yin, H. Wu and J. Wu, Multiscale structure engineering for high-performance Pb-free piezoceramics, *Acc. Mater. Res.* **3**, 461 (2022).
- <sup>26</sup>M. Waqar, H. Wu, J. Chen, K. Yao and J. Wang, Evolution from lead-based to lead-free piezoelectrics: Engineering of lattices, domains, boundaries, and defects leading to giant response, *Adv. Mater.* **34**, 2106845 (2022).
- <sup>27</sup>Z. Wang, K. G. Webber, J. M. Hudspeth, M. Hinterstein and J. E. Daniels, Electric-field-induced paraelectric to ferroelectric phase transformation in prototypical polycrystalline BaTiO<sub>3</sub>, *Appl. Phys. Lett.* **105**, 161903 (2014).
- <sup>28</sup>N. Novak, R. Pirc and Z. Kutnjak, Effect of electric field on ferroelectric phase transition in BaTiO<sub>3</sub> ferroelectric, *Ferroelectrics* **469**, 61 (2014).
- <sup>29</sup>M. H. Lente, A. Picinin, J. P. Rino and J. A. Eiras, 90-degree domain wall relaxation and frequency dependence of the coercive field in the ferroelectric switching process, *J. Appl. Phys.* **95**, 2646 (2004).
- <sup>30</sup>X. Wei, C. Zhao, T. Zheng and J. Wu, Decoding the relationship between the electrocaloric strength and phase structure in perovskite ferroelectrics towards high performance, *J. Mater. Chem. C* **9**, 2063 (2021).